Bioorganic & Medicinal Chemistry 19 (2011) 312–320

Contents lists available at ScienceDirect

Bioorganic & Medicinal Chemistry

journal homepage: www.elsevier.com/locate/bmc

Antimalarials based on the dioxane scaffold of plakortin. A concise synthesis and SAR studies

Caterina Fattorusso [a], Marco Persico [a], Nicoletta Basilico [b], Donatella Taramelli [b], Ernesto Fattorusso [a], Fernando Scala [a], Orazio Taglialatela-Scafati [a,*]

[a] Dipartimento di Chimica delle Sostanze Naturali, Università di Napoli 'Federico II', Via D. Montesano, 49, I-80131 Napoli, Italy
[b] Dipartimento di Sanità Pubblica-Microbiologia-Virologia, Università degli Studi di Milano, Via Pascal, 36 Milano, Italy

ARTICLE INFO

Article history:
Received 29 July 2010
Revised 8 November 2010
Accepted 8 November 2010
Available online 11 November 2010

Keywords:
Antimalarial
Endoperoxide
Plakortin
Knoevenagel reaction
Photooxygenation

ABSTRACT

In our search for new antimalarial agents inspired by natural products, we describe herein the synthesis, the evaluation of in vitro antiplasmodial activity, and the SAR studies for a series of endoperoxide antimalarials based on the plakortin scaffold. These simplified analogues are characterized by: (i) a 3,6-dihydro-1,2-dioxin ring or a 1,2-dioxane ring disubstituted at C-4 and C-5; (ii) a pentyl substituent at C-6 ('western' alkyl side chain) and they have been prepared from commercially available material using simple reactions.

1. Introduction

Malaria infections continue to be a global threat: about 40% of world population lives in endemic area and each year 350–500 million clinical episodes occur causing more than 2.0 million deaths. About 90% of these episodes are located in tropical Africa mainly in children under 5 years of age.[1] The growing of the malarial social and economic burden experienced in the last years has been attributed to population movements into malarial regions, climate change and, above all, to the proliferation of multi-drug resistant *Plasmodium falciparum* (Pf) parasites. This renders the control of malaria a particularly challenging task. Indeed, malaria affects mostly the poorest people of the world who do not have access to the effective antimalarial agents, while, on the other hand, the few low-cost drugs available are those for which malaria has developed resistance. Therefore, it is of primary importance to discover new antimalarial agents that can overcome these disadvantages. The recently reported presence of cases of artemisinin clinical resistance[2] and the new international campaign toward elimination of malaria has further reinforced this need.

Medicine for Malaria Venture (MMV) has published the Target Product Profile (TPP) of new antimalarial agents.[3] The TPP is a list of requirements that a new molecule should satisfy in order to be evaluated as clinical candidate; among these requirements, oral activity and a cost treatment of less than 1$ for uncomplicated malaria and 5$ for severe malaria are of particular significance.

In the course of our ongoing search for antimalarial lead compounds from marine sources, we have reported that plakortin (**1**) and its 9,10-dihydroderivative **2** (Chart 1), simple endoperoxide-containing polyketides isolated in good yields from the Caribbean sponge *Plakortis simplex*,[4] possess a significant in vitro antimalarial activity on CQ-resistant Pf strains.[5]

The isolation of plakortin analogues from the same[6] and related sources[7] and the preparation of a series of semi-synthetic plakortin derivatives[8] provided information about the structural requirements of the antimalarial activity of these simple 1,2-dioxanes. These results confirmed the crucial role of the endoperoxide functionality (the plakortin diol is completely inactive), suggested the importance of the 'western' alkyl side chain and revealed conformation-dependent features critical for antimalarial activity.[8]

In a recently reported investigation,[9] based on a combined chemical and computational approach, we have refined our knowledge on the possible mechanism of antimalarial action for molecules belonging to the plakortin family. Our investigation resulted in the proposal that, upon interaction with the Fe(II) (likely heme) center, and consequent formation of an oxygen-centered radical (preferentially O1), a simultaneous 'through space' 1,4 or 1,5 intramolecular radical shift to a western side chain carbon takes place (Figure 1). This yields to the formation of carbon radicals at the 'western' side chain which should be the toxic species giving intermolecular reactions with plasmodium molecular

* Corresponding author. Tel.: +39 081 678509; fax: +39 081 678552.
E-mail address: scatagli@unina.it (O. Taglialatela-Scafati).

0968-0896/$ - see front matter © 2010 Elsevier Ltd. All rights reserved.
doi:10.1016/j.bmc.2010.11.014

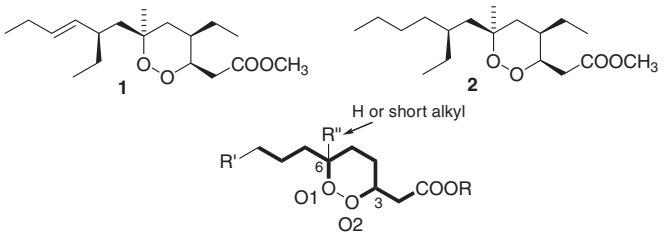

Chart 1. Plakortin (**1**) and dihydroplakortin (**2**) and the schematic structure of the plakortin pharmacophore.

targets. On the other hand, the presence of an additional iron interacting function, such as the ester group, appears to affect endoperoxide approach to heme. Thus, accessibility of the endoperoxide oxygens to the reactive iron species and correct orientation of reaction partners for the intramolecular radical shift with respect to O1, are essential requirements of the bioactive conformation.

In summary, the acquired information suggested that a simplified plakortin molecular scaffold, comprising the essential pharmacophoric portions, should include (Chart 1): (a) a dioxane ring; (b) a monosubstitution at position 3; (c) a mono- or disubstitution at position 6, which should guarantee the presence of an alkyl chain long enough to provide a partner for the above described intramolecular shift.

Following the above requirements, we have now synthesized simplified plakortin analogues starting from commercially available material and using simple reactions. The obtained molecules are characterized by (i) a 3,6-dihydro-1,2-dioxin ring or a 1,2-dioxane ring disubstituted at C-4 and C-5; (ii) a pentyl substituent at C-6 ('western' alkyl side chain); and (iii) an ester, a carboxyl or an hydroxyl group at C-3 ('eastern' side chain). In this paper we report the synthesis, the biological evaluation and the SARs studies for the novel series of antimalarials.

2. Results and discussion

2.1. Chemistry

The need for an easy and cheap synthesis addressed our interest toward the singlet oxygen addition to 1,3-butadiene derivatives for the construction of the endoperoxide ring, which represents the critical step of the synthetic procedure. This reaction, depicted in Scheme 1, yields 3,6-disubstituted 1,2-diox-4-ene derivatives and occurs readily on acyclic conjugated dienes.[10] Some aspects of the reaction mechanism[11,12] are worthy of being noted: (i) As shown in Scheme 1, the relative configuration of the product is directly dependent on the geometry of the reagent as a consequence of a pseudo-concerted mechanism of reaction with an oxygen addition in a *syn* fashion.[12] (ii) For reactions with butadienes, the dienophilic reactivity of $^1O_2$ surpasses the other two possible modes of reaction, which would afford hydroperoxides (even if allylic hydrogen atoms are present) and 1,2-dioxetanes. (iii) This reaction requires a *s-cis* conformation of the butadiene derivative and the *E,E* isomer, showing a higher population of the *s-cis* conformer at the equilibrium, reacts much faster than the *E,Z* and *Z,Z*

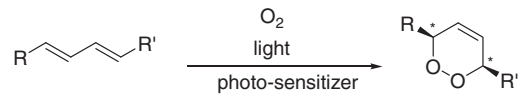

Scheme 1. A schematic view of the photooxygenation reaction of 1,3-butadienes. Asterisks indicate relative configurations.

isomers. (iv) Substituents *R* and *R′* (Scheme 1) should not be electron-withdrawing groups.[13]

On the basis of this available information, we planned to utilize the photo-oxygenation of *E,E*-alka-3,5-dienoic acid esters and to exploit the Ragoussis' modified Knoevenagel condensation[14,15] for its preparation. The most important features of this reaction, compared to the traditional Knoevenagel conditions, are the non-basic solvent (DMSO) and the presence of piperidinium acetate. These experimental conditions result in a minimization of the decarboxylative elimination of water, occurring in the Knoevenagel mechanism, while the dehydration of the hydroxylated intermediate to a non-conjugated β,γ-unsaturated dicarboxylic derivative is favored. The final decarboxylation of this intermediate yields an ester of alk-3-enoic acid (Scheme 2).

Thus, the commercially available *trans*-2-nonenal was allowed to react with ethyl hydrogen malonate in DMSO at 85 °C for 4 h in the presence of catalytic amounts of piperidinium acetate (Scheme 3). After work up, the mixture of obtained dienyl esters was further purified through repeated HPLC and argentation chromatography, to obtain pure ethyl undeca-3*Z*,5*E*-dienoate (**3**), ethyl undeca-3*E*,5*E*-dienoate (**4**), and trace amounts of the conjugated derivative **2**. Compound **4** was then subjected to photo-oxygenation reaction: a solution of **4** and methylene blue, as photo-sensitizer, in chloroform was irradiated under an oxygen atmosphere with a halogen lamp (500 W) for 24 h at −20 °C to afford in high yields (87%) the endoperoxide derivative **5**, as racemic mixture.

Given the laborious chromatographic procedure necessary to obtain the diene derivative **4** in the pure state, we attempted the photo-oxygenation reaction on the crude reaction product obtained from the modified Knoevenagel procedure described above. When the mixture was photo-oxygenated in the same conditions we obtained a mixture of the unreacted dienes **2** and **3** and the endoperoxide **5**, whose purification proved to be particularly simple. The yield of the target compound **5** was very similar to that obtained by photo-oxygenation of pure **4**. This outcome is in perfect agreement with the order of reactivity for dienyl esters: *E,E* (non-conjugated) > *Z,E* (non-conjugated) ≫ *E,E* (conjugated). Of course, in the search of an economically affordable procedure for the synthesis of simple antimalarial dioxanes, the elimination of a complex and low-yielding chromatographic step, unsuitable for large-scale low cost preparation, is an appreciable result.

Then, we prepared a series of derivatives of the endoperoxide **5** by reaction on both the ester and the endocyclic double bond functionalities. Following analogous reactions conducted for plakortin,[8] selective ester reduction to the corresponding alcohol **6** was accomplished with the use of $LiBH_4$ (Scheme 4). Standard acetylation of **6** gave the corresponding ester **7**, while LiOH-mediated hydrolysis of the ester group afforded the carboxylic acid derivative **8** in good yields (Scheme 4). Attempts of obtaining reaction of the ester group with an organometallic reagent (butyl

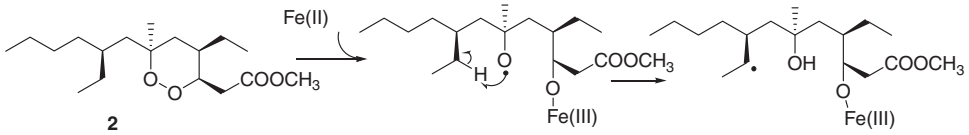

Figure 1. Mechanism proposed for the formation of the toxic side chain carbon radical for dihydroplakortin (**2**).

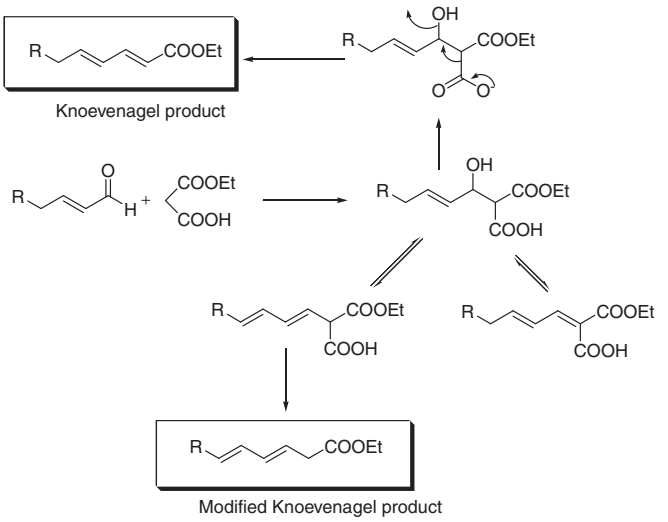

Scheme 2. The reported mechanism of the modified Knoevenagel reaction.

magnesium bromide) afforded, exclusively, attachment of the butyl group at one of the endoperoxide oxygen atoms, with consequent cleavage of the endoperoxide bond and formation of the ether derivative **9**, as major regioisomeric product (Scheme 4). A similar organometallic nucleophilic ring-opening has been reported previously for bicyclic endoperoxides.[16]

Reactions at the double bond of **5** afforded the derivatives shown in Scheme 5. Compound **5** was subjected to a K_2OsO_4-mediated dihydroxylation reaction, following a recently reported procedure aimed at asymmetric sugar synthesis.[17] This reaction produced, almost exclusively (>99% of diastereomeric excess), the racemic mixture of the single diastereomer **10** (stereostructure assigned by 2D NMR spectroscopy), as a result of the tendency of the hydroxylation reagent to add from the least hindered face. Compound **10** proved to be relatively unstable at room temperature and was kept at 0 °C. Treatment of **5** with *m*-CPBA in CH_2Cl_2 afforded a mixture of two compounds, which were purified through normal-phase HPLC. Extensive use of 1D and 2D NMR spectroscopy (particularly ROESY experiments were used for relative configurational assignments) allowed the identification of the diastereomeric epoxide derivatives **11** and **12**, corresponding to the products of the two possible *syn* approaches of the epoxidizing reagent to the double bond. Of course, both compounds were obtained as racemic mixtures. Analogously, bromination at the double bond afforded the two diastereomeric **13** and **14**.

Finally, we attempted chemoselective reduction of the double bond of **5**. Diimide-mediated reduction appeared to be the best candidate reaction to accomplish this transformation without affecting the endoperoxide bond.[18] Unfortunately, all our attempts, including in situ generation of diimide in different conditions (even with a 20-fold excess of potassium azodicarboxylate), proved to be unsuccessful. While diimide reduction has been reported for dioxene derivatives embedded in bicyclic systems,[18,19] as those deriving from singlet oxygenation of 1,3-cycloalkadienes, the same reaction is reported to be much less effective for simple monocyclic dioxin derivatives. Bascetta et al.[20] proposed an explanation of this different reactivity by considering that the approach of diimide to monocyclic endoperoxides such as **5**, either above or below the plane of the double bond, is hindered by an unfavorable electronic interaction between diimide and the non-bonding electron pairs

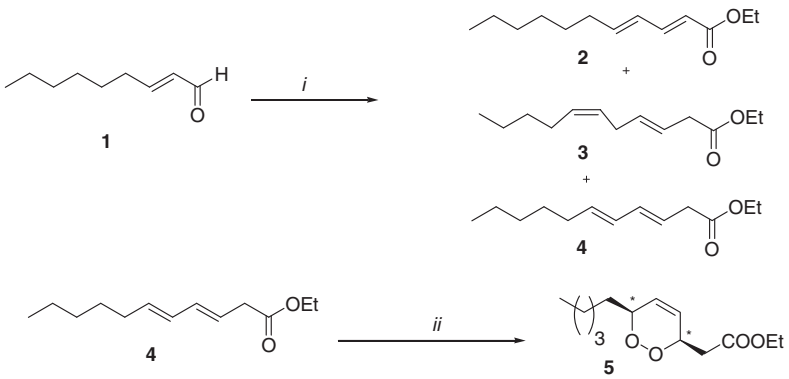

Scheme 3. Synthesis of the endoperoxide derivative **5** as racemic mixture. (i) Et/H malonate, piperidinium acetate in DMSO at 85 °C; (ii) O_2, light 500 W, methylene blue.

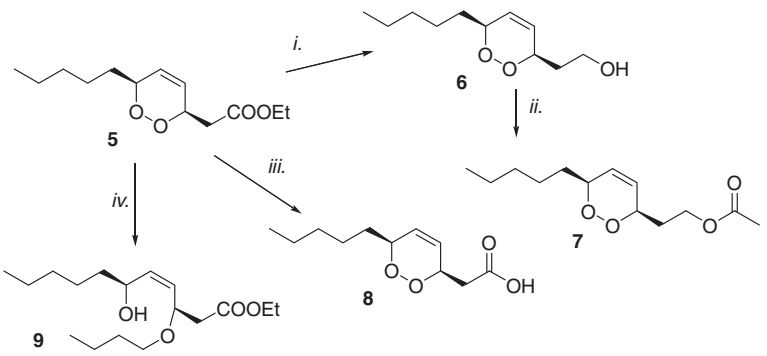

Scheme 4. Derivatives of the endoperoxide **5** prepared through reactions at the ester group. All the compounds were obtained as racemic mixtures. (i) $LiBH_4$; (ii) Ac_2O/pyr; (iii) LiOH/THF; (iv) BuMgBr.

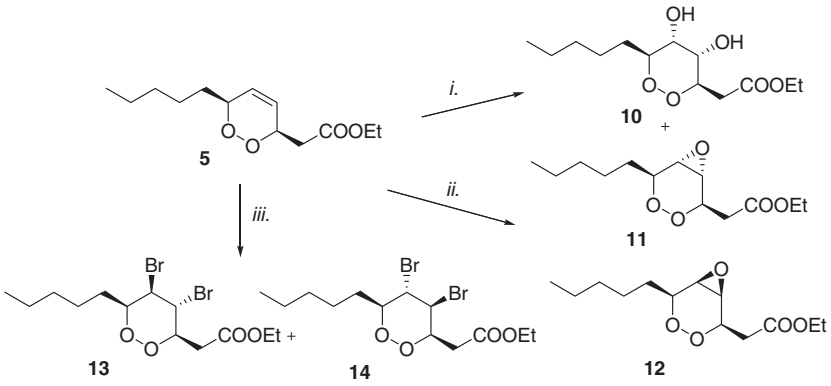

Scheme 5. Derivatives of the endoperoxide **5** prepared through reactions at the double bond. All the compounds were obtained as racemic mixtures. (i) K_2OsO_4; (ii) *m*-CPBA; (iii) Br_2.

on oxygen atoms. On the contrary, some bicyclic systems adopt a strained conformation allowing an approach of diimide which avoids interaction with oxygen electrons.

2.2. Structure–activity relationships

All the synthetic derivatives prepared in the course of this study have been evaluated for in vitro antimalarial activity against D10 (chloroquine-sensitive strain) and W2 (chloroquine-resistant strain). Results are reported in Table 1. Ring-opened derivative **9** showed no activity in the dose-range tested (Table 1) confirming, as reported for artemisinins[21] and plakortins,[8] that the endoperoxide ring system is critical for activity. Since conformation-dependent features resulted critical for antimalarial activity of plakortins,[8,9] a molecular modeling study has been performed to investigate the SARs of the novel series of antimalarials. The conformational space of **5–8** and **10–14** has been sampled through a combination of molecular dynamics, mechanic, and semi-empirical (PM6) quantum mechanical calculations (see Section 4.23 for details). Firstly, all the generated conformers were grouped on the basis of their ring conformation (Table 2) and ranked by their potential energy values. As reported in Table 2, the new endoperoxide scaffolds did not show a definite conformational preference for a specific 1,2-dioxane ring conformation, unlike **1** and **2**. In the case of these latter compounds, chair A represented the preferred conformation of the 1,2-dioxane ring, as well as the bioactive one, due to the 1,3-diaxal steric effect between the ethyl group at C-4 and the alkyl side chain at C-6. Then, we calculated the rate of low energy conformers (i.e., within 5 kcal/mol from the global minimum) owning required structural features for antimalarial activity of 1,2-dioxanes (putative bioactive conformers; Table 3; Figs. 2 and 3) according to our recently published model for the antimalarial activity;[9] that is: (i) the steric accessibility of the endoperoxide oxygens and (ii) the distance between the endoperoxide oxygen O1 and possible partners for a 'through space' (1,4 or 1,5) intramolecular radical shift (Table 3).

The most active compound of the series resulted compound **5**, which showed a good antimalarial activity (about one half of the plakortin potency, but about 100 times less potent than artemisinin) on both strains of *P. falciparum* (Table 1). This compound presented the same amount of low energy conformers which respected hypothesized pharmacophoric requirements for antimalarial activity with respect to **1** and around 70% of those of **2** (Table 3). Like already observed by us,[9] the higher reactivity of the 'western' side chain of **1** in a radical transfer reaction counterbalances its lower rate of putative bioactive conformers with respect to **2**. Accordingly, the observed activity of **5** is in agreement with its rate of bioactive conformers (23%, as **1**) and the lower reactivity of its side chain (as **2**). In addition, as stated above and unlike **1** and **2**, the putative bioactive conformers of **5** are distributed between the two possible half-chairs of the six-membered ring (Table 3). Since 1,2-dioxane and 1,2-dioxin ring conversion is energetically

Table 1
In vitro antimalarial activity of compounds **5–14** against D10 (CQ-S) and W2 (CQ-R) strains of *Plasmodium falciparum*

	D10 IC_{50} μM	W2 IC_{50} μM
1[a] (PLK)	0.87 ± 0.35	0.39 ± 0.13
2[a] (DHPLK)	0.90 ± 0.56	0.43 ± 0.16
5	1.20 ± 0.21	1.49 ± 0.22
6	>30	>30
7	21.90 ± 1.33	12.50 ± 2.51
8	3.33 ± 0.68	3.42 ± 0.56
9	>30	>30
10	>30	>30
11	22.10 ± 6.55	10.30 ± 3.21
12	>30	>30
13	8.15 ± 1.34	5.11 ± 0.98
14	9.12 ± 0.88	5.65 ± 1.22
Chloroquine	0.03 ± 0.01	0.25 ± 0.01

Data are means ± SD of four different experiments in triplicate.
[a] Data from Ref. 9.

Table 2
Occurrence rate (%) of 1,2-dioxane ring conformations considering PM6 conformers within 5 kcal/mol from the global minimum

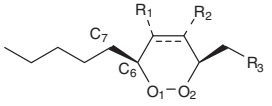

Compound	Chair A[a] (τ^b = 179.68°)	Chair B[a] (τ^b = −66.11°)	Boat A (τ^b = −83.53°)	Boat B (τ^b = −170.03°)
5	49	51	—	—
6	55	45	—	—
7	51	49	—	—
8	43	57	—	—
10	44	34	10	12
11	45	55	—	—
12	66	34	—	—
13	41	59	—	—
14	32	35	14	19
1	82	6	11	1
2	85	8	7	—

[a] Half-chair A (τ = −174.85°) and half-chair B (τ = −72.89°) in the case of compounds **5–8** and **11–12**.
[b] O2–O1–C6–C7.

Table 3
Rates of PM6 conformers of **1**, **2**, **5–8** and **10–14** owning interatomic distances suitable for a radical shift from O1 (⩽3 Å) and the steric accessibility of the endoperoxide oxygens. Occurrence rates and 1,2-dioxane ring conformations.

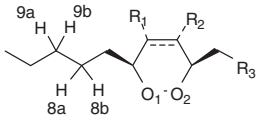

Compound	CNF[a] (%)	Chair A[b,c] (%)	Chair B[b,c] (%)	Boat A[b] (%)	Boat B[b] (%)
5	23	14	9	—	—
6	11	6	5	—	—
7	9	5	4	—	—
8	23	12	11	—	—
10	21	9	2	4	6
11	21	13	8	—	—
12	14	11	3	—	—
13	10	—	10	—	—
14	8	7	—	1	—
1	23	22	—	1	—
2	32	29	2.5	0.5	—

[a] Rate of conformers within 5 kcal/mol from the global minimum owning intramolecular distances suitable for a 1,4 or 1,5 H-shift from O1 to the 'western' side chain.
[b] Rate of conformers belonging to this family.
[c] Half-chair in the case of compounds **5–8** and **11–12**.

disfavored by the anomeric effect caused by the presence of two adjacent oxygens,[22] then the strong preference of **1** and **2** for a specific ring conformation, compared to **5** (Tables 2 and 3), likely affected the actual rate of putative bioactive conformers and, consequently, antimalarial activity.

All the synthetic derivatives prepared from **5** through modification of the ester group proved to be less active than their parent compound, but in different extent. Compound **8**, characterized by the same conformational properties of **5** (Tables 2 and 3), showed ~2.5-fold decreased activity against both *P. falciparum* strains (Table 1) due to the presence of a carboxylic function in place of the ester group of **5**, which unfavorably affects parasite penetration, like already observed for the corresponding plakortin derivative.[8] On the other hand, when a primary alcohol (**6**) or an oxyacetyl (**7**) group were introduced in place of the ester function (**5**), the resulting compounds showed a dramatic decrease of activity (Table 1). Calculations of solvent accessible (Connolly) surface revealed that endoperoxide oxygens lone pairs accessibility of **6** and **7** is impaired by the presence of an additional methylene at C-3 alkyl chain, lowering the rate of putative bioactive conformers to 11% and 9%, respectively (Table 3).

The addition of different substituents at the sp^2 carbons C-4 and C-5 (**10–14**), also determined a decrease of the antimalarial activity (Table 1). The 1,2-diol derivative (**10**) was completely inactive. Although **10** presented 21% of putative bioactive conformers, they all showed the endoperoxide function involved in a hydrogen bond network with the hydroxyl groups (Figure 2C). This suggests that the presence of the diol function could either interfere with iron binding or quench the oxygen-centered radicals formed by peroxide bond cleavage. Similar interferences can account for the low activity of epoxide derivatives **11** and **12**. It should be noted that the *trans*-epoxide derivative (**11**) is poorly active (sevenfold less active than **5**), but more than its *cis* counterpart (**12**) which is inactive in the range tested (Table 1), in agreement with their respective amount of putative bioactive conformers (Table 3). This also implies that the optimal spatial placement of the epoxide oxygen for the approach to heme is related to the position of the intramolecular reaction partner (Figure 3). Finally, when two bromine atoms were introduced at C-4 and C-5, the resulting compounds

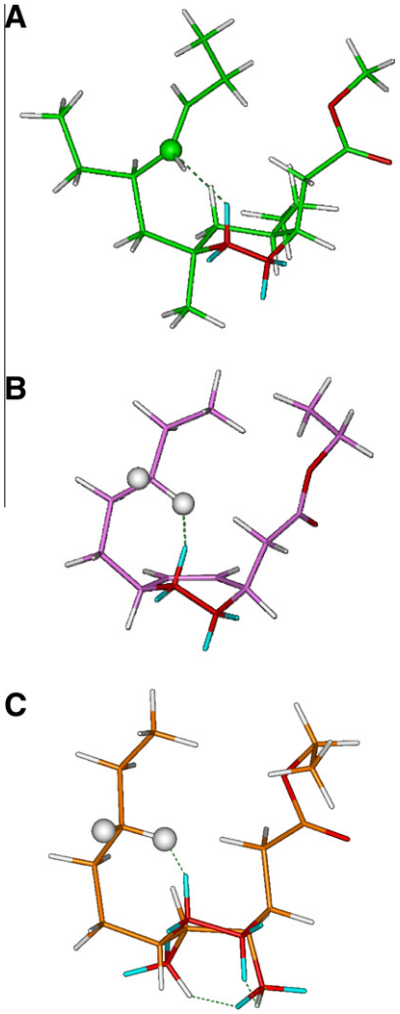

Figure 2. A putative bioactive conformer of plakortin (**1**) (A, green), **5** (B, pink), and **10** (orange). Molecules are colored by atom type (O = red, H = white and lone pairs = cyan). Possible partners in a 'through-space' intramolecular radical shift are evidenced as balls. Hydrogen bonds are highlighted by green dashed lines.

13 and **14** showed a similar antimalarial activity against both *P. falciparum* strains, but they were about fourfold less active than the parent compound **5** and about 13-fold than **1** (Table 1). The two diastereoisomers, showed a similar decreased amount of bioactive conformers with respect to **5** (Table 3) and, due to the steric hindrance of bromine atoms, presented, as bioactive 1,2-dioxane ring conformation, exclusively the chair with these atoms in equatorial position (i.e., chair B for **13** and chair A for **14**; Table 3). Moreover, it is likely that also the two bromine atoms could affect endoperoxide approach to heme iron.

In summary, the newly derived SARs confirmed our previously reported observations[8,9] about the importance of a definite preference for a specific conformation of the endoperoxide ring which allow the simultaneous endoperoxide oxygen lone pairs accessibility by iron and the correct orientation of the alkyl chain at C-6 for an intra-molecular radical shift reaction. In addition, they also highlighted the role of further functional groups able to interfere with heme interaction.

3. Conclusions

Basing on the plakortin pharmacophore, we have reported in this work the preparation of a new antimalarial compound (**5**), starting from commercially available materials and using a

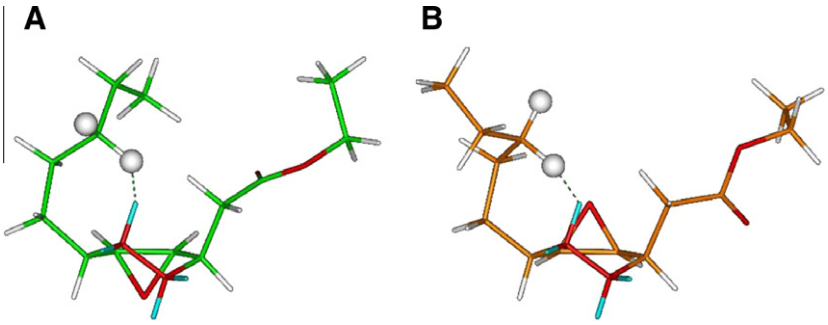

Figure 3. Putative bioactive conformer of **11** (A, green) and **12** (B, orange). Molecules are colored by atom type (O = red, H = white and lone pairs = cyan). Possible partners in a 'through-space' intramolecular radical shift are evidenced as balls.

sequence of two easy and cheap reactions (Scheme 3). Compound **5** showed an IC_{50} = 1.20 μM, about 100 times less potent in vitro than the natural and clinically used trioxane artemisinin. Although all the attempted modifications on the molecular scaffold of **5** caused a decrease in the pharmacological activity, the obtained SAR could drive the preparation of a number of further compounds of this series bearing different alkyl chains. These compounds could be prepared following the same reactions herein described but starting from different α,β-unsaturated aldehydes.

4. Experimental section

4.1. General

^1H (500 MHz) and ^{13}C (125 MHz) NMR spectra were measured on a Varian INOVA spectrometer. Chemical shifts were referenced to the residual solvent signal ($CDCl_3$: δ_H 7.26, δ_C 77.0). Homonuclear ^1H connectivities were determined by the COSY experiment; one-bond heteronuclear ^1H–^{13}C connectivities by the HSQC experiment; two- and three-bond ^1H–^{13}C connectivities by gradient-HMBC experiments optimized for a $^{2,3}J$ of 8 Hz. Through-space ^1H connectivities were evidenced by using a ROESY experiment with a mixing time of 500 ms. ESI-MS spectra were performed on a LCQ Finnigan MAT mass spectrometer. Medium pressure liquid chromatography was performed on a Büchi apparatus using a silica gel (230–400 mesh) column; HPLC were achieved on a Knauer apparatus equipped with a refractive index detector. The Knauer HPLC apparatus was used to purify and assess purity (>95%) of all final products. LUNA (normal phase, SI60, 250 × 4 mm) (Phenomenex) columns were used, with elution with EtOAc/*n*-hexane mixtures and 0.7 mL/min as the flow rate.

4.2. Modified Knoevenagel condensation

A solution of ethyl hydrogen malonate (5.0 g, 0.040 mol) and piperidinium acetate (36.8 mg, 0.26 mmol) in DMSO (20 mL) was stirred in a round-bottom flask for 15 min and then (*E*)-2-nonenal (3.4 mL, 0.026 mol) was added at once. Stirring was continued for 30 min and then the reaction mixture was heated slightly until 85 °C for 4 h, following the production of carbon dioxide. After cooling at room temperature, the reaction mixture was poured into cold water (40 mL) and extracted with diethyl ether (30 mL). The combined extracts were washed with water (3 × 40 mL) and dried over anhydrous Na_2SO_4 and the solvent removed under vacuum. The crude product was separated over silica column (eluent *n*-hexane/EtOAc 9:1) to give a mixture of ethyl undeca-3*Z*,5*E*-dienoate (**3**), ethyl undeca-3*E*,5*E*-dienoate (**4**), and ethyl undeca-2*E*,4*E*-dienoate (**2**). All the attempts to further purify this crude mixture over silica columns failed and also HPLC purifications gave no pure products. A portion of the obtained mixture was separated into its constituents through Ag^+-impregnated silica gel column, eluting with *n*-hexane/EtOAc mixtures from 95:5 to 8:2 and obtaining ethyl undeca-3*Z*,5*E*-dienoate (**3**, 1.64 g, 30% yield), ethyl undeca-3*E*,5*E*-dienoate (**4**, 2.07 g, 38% yield), and ethyl undeca-2*E*,4*E*-dienoate (**2**, 270 mg, 5% yield).

4.3. Ethyl undeca-2*E*,4*E*-dienoate (2)

Colorless oil. EIMS: *m/z* 210 $[M]^+$, HREIMS: *m/z* 210.1615, calcd for $C_{13}H_{22}O_2$ *m/z* 210.1620. ^1H NMR ($CDCl_3$): δ 7.30 (H-3, dd, *J* = 15.5, 11.0 Hz); 5.94 (H-2, d, 15.5 Hz); 5.86 (H-4, dd, *J* = 15.5, 11.0 Hz); 5.68 (H-5, dt, *J* = 15.5, 7.5 Hz); 4.10 (OCH_2, q, *J* = 7.3 Hz); 2.20 (H-6, m); 1.30–1.20 (H_2-7, H_2-8, H_2-9, H_2-10, m); 1.15 (OCH_2CH_3, t, *J* = 7.3 Hz); 0.90 (H_3-11, t, *J* = 7.3 Hz).

4.4. Ethyl undeca-3*E*,5*Z*-dienoate (3)

Colorless oil. EIMS: *m/z* 210 $[M]^+$, HREIMS: *m/z* 210.1613, calcd for $C_{13}H_{22}O_2$ *m/z* 210.1620. ^1H NMR ($CDCl_3$): δ 6.42 (H-4, dd, *J* = 15.2, 11.0 Hz); 5.98 (H-5, dd, 11.0, 10.7 Hz); 5.73 (H-6, dt, *J* = 7.7, 7.5 Hz); 5.42 (H-3, dt, *J* = 11.0, 6.7 Hz); 4.10 (OCH_2, q, *J* = 7.3 Hz); 3.13 (H-2, d, 6.7 Hz); 2.16 (H-7, m); 1.30–1.20 (H_2-8, H_2-9, H_2-10, m); 1.15 (OCH_2CH_3, t, *J* = 7.3 Hz); 0.88 (H_3-11, t, *J* = 7.3 Hz).

4.5. Ethyl undeca-3*E*,5*E*-dienoate (4)

Colorless oil. EIMS: *m/z* 210 $[M]^+$, HREIMS: *m/z* 210.1627, calcd for $C_{13}H_{22}O_2$ *m/z* 210.1620. ^1H NMR ($CDCl_3$): δ 6.08 (H-4, dd, *J* = 15.1, 10.3 Hz); 5.99 (H-5, dd, 15.1, 10.3 Hz); 5.64 (H-6, m); 5.56 (H-3, dt, *J* = 15.1, 7.0 Hz); 4.10 (OCH_2, q, *J* = 7.2 Hz); 3.06 (H-2, d, *J* = 7.0 Hz); 2.05 (H-7, m); 1.30–1.20 (H_2-8, H_2-9, H_2-10, m); 1.15 (OCH_2CH_3, t, *J* = 7.2 Hz); 0.88 (H_3-11, t, *J* = 7.0 Hz). ^{13}C NMR ($CDCl_3$): δ 172.0 (C-1); 135.3 (C-6); 134.2 (C-4); 129.5 (C-5); 122.5 (C-3); 61.0 (OCH_2CH_3); 38.0 (C-2); 29.7–29.5 (C-8; C-9; C-10); 25.7 (C-7); 14.6 (OCH_2CH_3); 14.1 (C-11).

4.6. Photo-oxygenation reaction

A solution of compound **4** (500 mg, 2.38 mmol) in $CHCl_3$/MeOH 95:5 (120 mL) was photolyzed with a 500 W halogen lamp in the presence of methylene blue (0.6 mg) as photosensitizer, through which was bubbled a constant stream of oxygen at a flow rate of 50 mL/min for 24 h. The reaction was performed in a Pyrex flask fitted with an external cooling jacket. The reaction mixture was then concentrated in vacuo and the resulting residue was purified by column chromatography (*n*-hexane/EtOAc mixtures from 99:1 to 9:1) to yield pure compound **5** (508 mg, 87% yield). When the same reaction was repeated in the same conditions for the mixture of dienes **2–4**, after chromatographic purification the single endoperoxide **5** was obtained.

4.7. Compound 5

Colorless oil. EIMS: *m/z* 242 $[M]^+$, HREIMS: *m/z* 242.1515, calcd for $C_{13}H_{22}O_4$ *m/z* 242.1518. ^1H NMR ($CDCl_3$): δ 5.93 (H-4, overlapped); 5.91 (H-5, overlapped); 4.83 (H-3, m); 4.60 (H-6, m); 4.08 (OCH_2, q, J = 7.2 Hz); 2.85 (H-2a, dd, J = 12.5, 7.3 Hz); 2.60 (H-2b, dd, J = 12.5, 3.5 Hz); 1.56 (H_2-7, m); 1.25-1.20 (H_2-8, H_2-9, H_2-10, m); 1.15 (OCH_2CH_3, overlapped); 0.88 (H_3-11, t, J = 7.0 Hz). ^{13}C NMR ($CDCl_3$): δ 170.8 (C-1); 129.5 (C-5); 126.7 (C-4); 78.6 (C-6); 75.2 (C-3); 61.0 (OCH_2CH_3); 38.8 (C-2); 32.7 (C-7); 32.0 (C-10); 22.8 (C-8; C-9); 14.6 (OCH_2CH_3); 14.4 (C-11).

4.8. $LiBH_4$-mediated reduction of compound 5 and acetylation of 6

Compound **5** (12.0 mg, 0.050 mmol) was dissolved in 0.8 mL of dry THF under argon flow at 0 °C and then 150 μL of a 2 M solution of $LiBH_4$ in THF (0.3 mmol) and 10 μL of dry MeOH were added dropwise to the solution. The reaction was kept under stirring for 2 h at 0 °C. Then, 10 μL of 1 M aqueous NaOH were added to the obtained mixture, which was partitioned between water and $CHCl_3$. The organic phase, dried with Na_2SO_4 and concentrated in vacuo was purified by HPLC (eluent *n*-hexane/EtOAc 75:25) affording pure compound **6** (9.0 mg, 0.045 mmol, 90% yield). Compound **6** (3.0 mg, 0.015 mmol) was dissolved in dry pyridine (1 mL) and treated with Ac_2O (1 mL). After standing overnight, the reaction was worked up by addition of a few drops methanol to destroy the excess Ac_2O, water (ca. 3 mL) and EtOAc (ca. 10 mL). The organic phase was washed sequentially with 2 N H_2SO_4, saturated $NaHCO_3$ and brine. After drying (Na_2SO_4) and removal of the solvent, 3.0 mg (0.012 mmol, 80% yield) of compound **7** were obtained.

4.9. Compound 6

Colorless solid. EIMS: *m/z* 200 $[M]^+$, HREIMS: *m/z* 200.1422, calcd for $C_{11}H_{20}O_3$ *m/z* 200.1412. ^1H NMR ($CDCl_3$): δ 5.90 (H-4, overlapped); 5.90 (H-5, overlapped); 4.63 (H-3, m); 4.55 (H-6, m); 3.80 (H_2-1, m); 1.88 (H_2-2, m); 1.62 (H_2-7, m); 1.31 (H_2-8, H_2-9, H_2-10, m); 0.88 (H_3-11, t, J = 7.0 Hz).

4.10. Compound 7

Colorless solid. EIMS: *m/z* 200 $[M]^+$, HREIMS: *m/z* 200.1527, calcd for $C_{13}H_{22}O_4$ *m/z* 200.1518. ^1H NMR ($CDCl_3$): δ 5.91 (H-4, overlapped); 5.91 (H-5, overlapped); 4.58 (H-3, overlapped); 4.58 (H-6, overlapped); 4.22 (H_2-1, m); 2.08 (CH_3CO, s); 1.92 (H_2-2, m); 1.62 (H_2-7, m); 1.31 (H_2-8, H_2-9, H_2-10, m); 0.88 (H_3-11, t, J = 7.0 Hz).

4.11. Hydrolysis of compound 5

Compound **5** (9.0 mg, 0.037 mmol) was dissolved in a THF/H_2O 3:1 solution (3.0 mL) and 4 mg of LiOH were added. The solution was stirred at 0 °C overnight. Then, the reaction mixture was partitioned between EtOAc and water. The organic phase, evaporated to dryness, contained compound pure compound **8** (7.0 mg, 0.033 mmol, 89% yield).

4.12. Compound 8

Colorless oil. EIMS: *m/z* 214 $[M]^+$, HREIMS: *m/z* 214.1215, calcd for $C_{13}H_{22}O_4$ *m/z* 214.1205. ^1H NMR (500 MHz, CD_3OD): δ 5.90 (H-4, d, J = 2.5 Hz); 5.68 (H-5, d, J = 2.5 Hz); 5.15 (H-3, m); 4.95 (H-6, m); 2.75 (H-2a, dd, J = 12.5, 7.5 Hz); 2.55 (H-2b, dd, J = 12.5, 3.7 Hz); 1.56 (H_2-7, m); 1.25-1.20 (H_2-8, H_2-9, H_2-10, m); 0.88 (H_3-11, t, J = 7.0 Hz).

4.13. Treatment of compound 5 with BuMgBr

Compound **5** (18.0 mg, 0.074 mmol) was dissolved in 5 mL THF and chilled to -78 °C under argon. Butyl magnesium bromide (0.105 mmol) solution in THF was added dropwise and the reaction mixture was allowed to warm to 0 °C over 1 hr. The resulting solution was poured into a separatory funnel containing 20 mL of Et_2O and 10 mL of saturated ammonium chloride. The aqueous layer was extracted with CH_2Cl_2 and Et_2O and the combined organic layers purified by HPLC (eluent *n*-hexane/EtOAc 75:25) affording compound **9** (10.2 mg, 0.034 mmol, 46% yield) as major product.

4.14. Compound 9

Colorless amorphous solid. EIMS: *m/z* 300 $[M]^+$, HREIMS: *m/z* 300.2309, calcd for $C_{17}H_{32}O_4$ *m/z* 300.2301. ^1H NMR (500 MHz, $CDCl_3$): δ 5.60 (H-5, m); 5.38 (H-4, m); 4.58 (H-3, m); 4.50 (H-6, m); 3.50, 3.30 (-OCH_2, m), 2.67 (H-2a, m); 2.42 (H-2b, m); 1.60 (H_2-7, -OCH_2CH_2, m); 1.30–1.20 (H_2-8, H_2-9, H_2-10, -$OCH_2CH_2CH_2CH_3$, m); 0.90 (-$OCH_2CH_2CH_2CH_3$, H_3-11, t, J = 7.0 Hz).

4.15. Dihydroxylation of compound 5

To a stirred solution of compound **5** (10 mg, 0.042 mmol) in *t*-BuOH (2.5 mL) and water (2.5 mL) was added K_2OsO_4 (0.5 mol %) and citric acid, followed by NMO (5.1 mg). The mixture was stirred for 3 h and followed by TLC. Then, the reaction mixture was extracted with CH_2Cl_2, dried over Na_2SO_4 concentrated in vacuo and the product purified by HPLC (normal phase *n*-hexane/EtOAc 1:1) to obtain compound **10** (8.1 mg, 0.029 mmol, 69% yield).

4.16. Compound 10

Colorless solid. EIMS: *m/z* 276 $[M]^+$, HREIMS: *m/z* 276.1579, calcd for $C_{13}H_{24}O_6$ *m/z* 276.1573. ^1H NMR ($CDCl_3$): δ 4.59 (H-3, m); 3.79 (H-6, m); 3.68 (H-4, overlapped); 3.61 (H-5, m); 4.08 (OCH_2CH_3, q, J = 7.2 Hz); 2.78 (H-2a, dd, J = 12.1, 7.2 Hz); 2.60 (H-2b, dd, J = 12.1, 3.5 Hz); 1.60 (H_2-7, m); 1.25-1.20 (H_2-8, H_2-9, H_2-10, m); 1.15 (OCH_2CH_3, overlapped); 0.88 (H_3-11, t, J = 7.0 Hz).

4.17. Epoxidation of compound 5

Compound **5** (18.0 mg, 0.074 mmol) was dissolved in 2.5 mL of dry CH_2Cl_2 and 130 mg of *meta*-chloroperbenzoic acid (0. 74 mmol) were added to the solution that was then stirred overnight at room temperature. Subsequently, the reaction mixture was partitioned between $CHCl_3$ and saturated aqueous $NaHCO_3$. The organic phase, dried and concentrated in vacuo, was then purified by reversed-phase HPLC (eluent MeOH/H_2O 9:1) yielding compounds **11** (9.6 mg, 0.037 mmol, 50% yield) and **12** (2.5 mg, 0.0097 mmol, 13% yield) in the pure state.

4.18. Compound 11

Colorless solid. EIMS: *m/z* 258 $[M]^+$, HREIMS: *m/z* 258.1477, calcd for $C_{13}H_{22}O_5$ *m/z* 258.1467. ^1H NMR (CD_3OD): δ 4.76 (H-3, m); 4.30 (H-6, m); 3.60 (H-4, m); 3.32 (H-5, m); 4.18 (OCH_2, q, J = 7.2 Hz); 2.90 (H_2-2, m); 1.60 (H_2-7, m); 1.45 (H_2-8, m); 1.33-1.30 (H_2-9, H_2-10, m); 1.30 (OCH_2CH_3, overlapped); 0.90 (H_3-11, t, J = 7.0 Hz). ^{13}C NMR ($CDCl_3$): δ 170.8 (C-1); 83.7 (C-6); 74.1 (C-3); 60.7 (OCH_2CH_3); 51.5 (C-4); 48.9 (C-5); 37.5 (C-2); 32.0 (C-7); 32.8 (C-8; C-9); 23.5 (C-10); 14.1 (C-11); 13.4 (OCH_2CH_3).

4.19. Compound 12

Colorless solid. EIMS: *m/z* 258 $[M]^+$, HREIMS: *m/z* 258.1473, calcd for $C_{13}H_{22}O_5$ *m/z* 258.1467. ^1H NMR (CD_3OD): δ 4.70 (H-3,

m); 4.37 (H-6, m); 3.37 (H-4, m); 3.25 (H-5, m); 4.13 (OCH_2, q, J = 7.2 Hz); 2.92 (H-2a, dd, J = 12.5, 6.4 Hz); 2.78 (H-2b, dd, J = 12.5, 3.2 Hz); 1.62 (H_2-7, m); 1.45 (H_2-8, m); 1.33–1.30 (H_2-9, H_2-10, m); 1.29 (OCH_2CH_3, overlapped); 0.90 (H_3-11, t, J = 7.0 Hz). ^{13}C NMR ($CDCl_3$): δ 170.4 (C-1); 78.8 (C-6); 74.7 (C-3); 61.2 (OCH_2CH_3); 51.3 (C-4); 47.9 (C-5); 36.0 (C-2); 32.0 (C-7); 32.1 (C-8; C-9); 23.0 (C-10); 14.1 (C-11); 13.4 (OCH_2CH_3).

4.20. Bromination of compound 5

Bromine (12.5 mg, 0.078 mmol) was added in the dark to a solution of compound **5** (15 mg, 0.062 mmol) in CH_2Cl_2 (2.0 mL) in a vial kept at 0 °C. After 15 min the solvent was removed under a stream of nitrogen and the residue was purified by HPLC (normal phase *n*-hexane/EtOAc 85:15) to yield compounds **13** (16.3 mg, 0.041 mmol, 66.1% yield) and **14** (7.1 mg, 0.018 mmol, 29% yield).

4.21. Compound 13

Colorless solid. EIMS: *m/z* 400 $[M]^+$, HREIMS: *m/z* 399.9888, calcd for $C_{13}H_{22}{}^{79}Br_2O_4$ *m*/z 399.9885. ^{1}H NMR ($CDCl_3$): δ 5.17 (H-3, m); 4.80 (H-4, m); 4.32 (H-5, m); 4.18 (H-6, m); 4.10 (OCH_2, q, J = 7.2 Hz); 2.82 (H-2a, dd, J = 12.5, 6.0 Hz); 2.72 (H-2b, dd, J = 12.5, 2.5 Hz); 1.45 (H_2-7, m); 1.33–1.30 (H_2-8, H_2-9, H_2-10, m); 1.20 (OCH_2CH_3, overlapped); 0.92 (H_3-11, t, J = 7.0 Hz).

4.22. Compound 14

Colorless solid. EIMS: *m/z* 400 $[M]^+$, HREIMS: *m/z* 399.9882, calcd for $C_{13}H_{22}{}^{79}Br_2O_4$ *m*/z 399.9885. ^{1}H NMR ($CDCl_3$): δ 4.84 (H-3, m); 4.25 (H-6, m); 4.20 (H-4, m); 3.80 (H-5, m); 4.10 (OCH_2, q, J = 7.2 Hz); 2.92 (H-2a, dd, J = 12.5, 5.8 Hz); 2.88 (H-2b, dd, J = 12.5, 3.5 Hz); 1.48 (H_2-7, m); 1.33–1.30 (H_2-8, H_2-9, H_2-10, m); 1.20 (OCH_2CH_3, overlapped); 0.90 (H_3-11, t, J = 7.0 Hz).

4.23. Molecular modeling

Molecular modeling calculations were performed on SGI Origin 200 8XR12000 and E4 Server Twin 2 x Dual Xeon—5520, equipped with two nodes. Each node: 2 x Intel® Xeon® QuadCore E5520—2,26Ghz, 36 GB RAM. The molecular modeling graphics were carried out on SGI Octane 2 workstations. The estimation of apparent pK_a values of the newly designed compounds were calculated by using the ACD/pK_a DB version 12.00 software (Advanced Chemistry Development Inc., Toronto, Canada). Compound **8** was considered deprotonated, while all the others compounds were considered neutral in all calculations performed, as a consequence of the estimation of percentage of neutral/ionized forms computed at the pH of 7.4 (physiological value) 7.2 (cytoplasmic pH value) and 5.5 (parasite vacuole pH) using the Handerson–Hasselbach equation. Compounds **5**–**8** and **10**–**14** were built using the Insight 2005 Builder module (Accelrys Software Inc., San Diego). Atomic potentials and charges were assigned using the CFF91 force field.[23] The conformational space of the compounds was sampled through 200 cycles of Simulated Annealing (ε = 1) applying the following protocol: the system was heated up to 1000 K over 2000 fs (time step = 3.0 fs); the temperature of 1000 K was applied to the system for 2000 fs (time step = 3.0 fs) with the aim of surmounting torsional barriers; successively temperature was linearly reduced to 300 K in 1000 fs (time step = 1.0 fs). Resulting structures were subjected to energy minimization within Insight 2005 Discover module (CFF91 force field; ε = 1) until the maximum RMS derivative was less than 0.001 kcal/Å, using Conjugate Gradient[24] as minimization algorithm. All conformers, obtained from molecular dynamics and mechanics calculations, were subjected to a full geometry optimization by semiempirical calculations, using the quantum mechanical method PM6[25] in the Mopac2009 package[26] and EF[27] (Eigenvector Following routine) as geometry optimization algorithm. GNORM value was set to 0.01. To reach a full geometry optimization the criteria for terminating all optimizations was increased by a factor of 100, using the keyword PRECISE. Resulting conformers were grouped into families on the base of their 3,6-dihydro-1,2-dioxine ring (**5**–**8**) or 1,2-dioxane ring (**10**–**14**) conformation and ranked by their potential energy values (i.e., ΔE from the global energy minimum). Occurrence rates, together with the distance between O1 and possible partners for a 'through space' (1,4 and 1,5) intramolecular radical shift, were calculated for all conformers within 5 kcal/mol from the global minimum. The accessible surface area of endoperoxide oxygens lone pairs has been evaluated by calculating Connolly surfaces (Insight 2005, Accelrys Software Inc., San Diego).

4.24. In vitro drug susceptibility assay on *P. falciparum*

The CQ-sensitive (D10) and the CQ-resistant (W2) strains of *P. falciparum* were cultured in vitro as described by Trager and Jensen.[28] Parasites were maintained in human type A-positive red blood cells at 5% hematocrit in RPMI 1640 (Gibco BRL, $NaHCO_3$ 24 mM) medium with the addition of 1% AlbuMaxII (Invitrogen, Milano, Italy), 0.01% hypoxanthine, 20 mM Hepes (Euroclone) and 2 mM glutamine (Euroclone). The cultures were maintained at 37 °C in a standard gas mixture consisting of 1% O_2, 5% CO_2, and 94% N_2. Test compounds were dissolved in either water or DMSO and then diluted with medium to achieve the required concentrations (final DMSO concentration <1%, which is non-toxic to the parasite). Compounds were placed in serial dilutions to 96 well flat-bottom microplates (COSTAR). Asexual parasite stages derived from asynchronous cultures with parasitemia of 1–1.5% were aliquoted into the plates (final hematocrit 1%) and incubated for 72 h at 37 °C. Parasite growth was determined spectrophotometrically (OD_{650}) by measuring the activity of the parasite lactate dehydrogenase (LDH), according to a modified version of Makler's method in control and treated cultures.[29] Chloroquine was used as reference control. The antiplasmodial activity is expressed as the 50% inhibitory concentrations (IC_{50}). Each IC_{50} value presented in Table 1 is the mean and standard deviation of three separate experiments performed in triplicate.

Acknowledgments

This work was supported by the FP6-EU Project 18834-AntiMal and by MIUR (PRIN2008: Leads ad Attività Antimalarica di Origine Naturale: Isolamento, Ottimizzazione e Valutazione Biologica). We thank the Associazione Volontari Italiani Sangue (AVIS Comunale Milano) for providing fresh red blood cells for *P. falciparum* growth. Mass and NMR spectra were recorded at the 'Centro di Ricerca Interdipartimentale di Analisi Strumentale' of the University of Naples 'Federico II'. The assistance of the staff is gratefully acknowledged.

References and notes

1. Snow, R. W.; Guerra, C. A.; Noor, A. M.; Myint, H. Y.; Hay, S. I. *Nature* **2005**, *434*, 214.
2. Dondorp, A. M.; Yeung, S.; White, L.; Nguon, C.; Day, N. P.; Socheat, D.; von Seidlein, L. *Nat. Rev. Microbiol.* **2010**, *8*, 272.
3. http://www.MMV.org/IMG/pdf/PRODUCT_PROFILE_with-logo.pdf.
4. Cafieri, F.; Fattorusso, E.; Taglialatela-Scafati, O.; Ianaro, A. *Tetrahedron* **1999**, *55*, 7045.
5. Fattorusso, E.; Parapini, S.; Campagnuolo, C.; Basilico, N.; Taglialatela-Scafati, O.; Taramelli, D. *J. Antimicrob. Chemother.* **2002**, *50*, 883.
6. Campagnuolo, C.; Fattorusso, E.; Romano, A.; Taglialatela-Scafati, O.; Basilico, N.; Parapini, S.; Taramelli, D. *Eur. J. Org. Chem.* **2005**, 5077.
7. Fattorusso, C.; Persico, M.; Calcinai, B.; Cerrano, C.; Parapini, S.; Taramelli, D.; Novellino, E.; Romano, A.; Scala, F.; Fattorusso, E.; Taglialatela-Scafati, O. *J. Nat. Prod.* **2010**, *73*, 1138.

8. Fattorusso, C.; Campiani, G.; Catalanotti, B.; Persico, M.; Basilico, N.; Parapini, S.; Taramelli, D.; Campagnuolo, C.; Fattorusso, E.; Romano, A.; Taglialatela-Scafati, O. *J. Med. Chem.* **2006**, *49*, 7088.
9. Taglialatela-Scafati, O.; Fattorusso, E.; Romano, A.; Scala, F.; Barone, V.; Cimino, P.; Stendardo, E.; Catalanotti, B.; Persico, M.; Fattorusso, C. *Org. Biomol. Chem.* **2010**, *8*, 846.
10. Matsumoto, M.; Kondo, K. *J. Org. Chem.* **1975**, *40*, 2259.
11. Clennan, E. L.; Mehrsheikh-Mohammadi, M. E. *J. Am. Chem. Soc.* **1983**, *105*, 5932.
12. Bobrowski, M.; Liwo, A.; Oldziej, S.; Jeziorek, D.; Ossowski, T. *J. Am. Chem. Soc.* **2000**, *122*, 8112.
13. Matsumoto, M.; Kuroda, K. *Tetrahedron Lett.* **1982**, *23*, 1285.
14. Ragoussis, N.; Ragoussis, V. *J. Chem. Soc., Perkin Trans. 1* **1998**, 3529.
15. Ragoussis, V.; Panopoulou, M.; Ragoussis, N. *J. Agric. Food Chem.* **2004**, *52*, 5047.
16. Schwaebe, M. K.; Little, R. D. *Tetrahedron Lett.* **1996**, *37*, 6635.
17. Robinson, T. V.; Taylor, D. K.; Tiekink, E. R. T. *J. Org. Chem.* **2006**, *71*, 7236.
18. Kepler, J. A.; Philip, A.; Lee, Y. W.; Morey, M. C.; Carroll, F. I. *J. Med. Chem.* **1988**, *31*, 713.
19. Bloodworth, A. J.; Eggelte, H. J. *J. Chem. Soc., Perkin Trans. 2* **1984**, 2069.
20. Bascetta, E.; Gunstone, F. D.; Scrimgeour, C. M. *J. Chem. Soc., Perkin Trans 1* **1984**, 2199.
21. Jefford, C. W. *Curr. Med. Chem.* **2001**, *8*, 1803.
22. (a) Freeman, F.; Po, H. N.; Hehre, W. J. *J. Mol. Struct. (Theochem)* **2000**, *503*, 145; (b) Freeman, F.; Lee, C.; Hehre, W. J.; Po, H. N. *J. Comput. Chem.* **1997**, *18*, 1392.
23. Maple, J. R.; Hwang, M. J.; Stockfisch, T. P.; Dinur, U.; Waldman, M.; Ewig, C. S.; Hagler, A. T. *J. Comput. Chem.* **1994**, *15*, 162.
24. Fletcher, R. Unconstrained Optimization In *Practical Methods of Optimization*; John Wiley & Sons: New York, 1980; Vol. 1.
25. Stewart, J. J. P. *J. Mol. Model.* **2007**, *13*, 1173.
26. MOPAC2009, James, J. P. Stewart, Stewart Computational Chemistry, Colorado Springs, CO, USA, http://OpenMOPAC.net, 2008.
27. Baker, J. *J. Comput. Chem.* **1986**, *7*, 385.
28. Trager, W.; Jensen, J. B. *Science* **1976**, *193*, 673.
29. Makler, M.; Hinrichs, D. *Am. J. Trop. Med. Hyg.* **1993**, *48*, 205.